

A Multi-Scale Theoretical Scheme for Metal Deformation

Robb Thomson, Retired,¹ L. E. Levine,¹ Y. Shim,² M. F. Savage,¹ and D. E. Kramer¹

Abstract: A conceptual theoretical scheme for single crystal metal deformation is presented consisting of multi-scale models from dislocation dynamics to the continuum constitutive relations. The scheme rests on the fundamental observations that deformation is characterized by partially ordered internal dislocation wall structures, discontinuous strain bursts in time, and strain localization in a surface slip band structure. A percolation strain model corresponds to elementary slip line burst events, with percolation parameters to be supplied from experiments and dislocation dynamics studies of wall structures. A model for localization of the slip lines into bands is proposed (for suitable loadings) which envisions channels for slip formed from the dense planar walls (otherwise called GNB's). A rudimentary continuum model is constructed from the outputs of these models which consists of two principal internal variables, and exhibits the desired hardening behavior with strain. The continuum model is based on two different material properties in the slip bands, and in the matrix between the bands. The scheme does not yet include mechanisms for the underlying dislocation ordering or patterning, but addresses the transport of dislocations through these (presumably known) structures.

1 Introduction

Over the past several years, the subject of deformation in metals has experienced a significant revival in interest. In large part, this was due to the development of the dislocation dynamics approaches[DeVinere and Kubin(1994); Zbib, Rhee and Hirth(1998); Ghoneim and Sun(1996); Schwartz(1999)] which modern computer technology makes possible. But new experimental techniques, [Ungar(2001); Zolotoyabko, Shilo and Lakin(2001); Blavette, Cadel and Fraczkiewicz(1999); DeHosson(2001); Wilkin-

son(1996); Chung and Ice(1999); Long, Levine, and Thompson(2000)] as well as other theoretical approaches have also been developed[Hahner(1996); El-Azab(2000); Zaiser(2001)]. Our own contribution to new theory was the strain percolation model proposed by two of us several years ago, and whose mathematical features have been developed in subsequent publications [Thomson and Levine(2000); Thomson, Levine and Stauffer(2000); Shim, Levine, and Thomson]. In the current paper, we will present a conceptual and partially quantitative view of how the percolation strain model relates to observed metallic deformation, and propose a linked set of models which can eventually carry one from the dislocation cell structure to a continuum constitutive law. Not surprisingly, we have not worked out the full details of such a linked set of models, but some of the links from one level to another are in place, and others look plausible and practicable. This paper is therefore presented as a tentative map and conceptual outline for achieving such a result, and from it one can begin to prioritize the work still required.

The fundamental premise in our work is that deformation is at its heart a stochastic nonequilibrium process, so the statistical physics point of view is particularly useful. We have not addressed the problem of how the dislocations become partially ordered as deformation proceeds, because of the great difficulty of such a project, but have been content to take the dislocation structures as given, and then develop a description of how dislocation transport takes place through this structure. As it turns out, even though the mechanisms which control the actual formation of the structures are not addressed, once a theoretical description of the transport is in hand, the evolution of the structure can be at least partially addressed.

2 Fundamental Features.

There are several features of metallic deformation which are so central to the phenomenon that they must be incor-

¹Metallurgy Division, NIST, Gaithersburg, MD 20877

²Center for Simulation Physics, University of Georgia, Athens, GA 30602

porated in any theory, and we begin with a short listing of them.

2.1 Cell Patterns.

The most obvious feature is the fact that the dislocations order themselves into two distinct classes of wall structures [Mughrabi, Ungar, Kienle and Wilkens(1986); Barlow, Bay and Hansen(1985); Pantleon and Hansen; Winther, Huang Hansen(2000); Hughes, Liu, Chrzan and Hansen(1997)]. The first have been called Incidental Dislocation Boundaries (IDB) [Barlow, Bay and Hansen (1985)]. These boundaries begin to develop in late Stage II, and are fully formed in Stage III.

A second class of cell wall (denser than the IDB) which appears when the load axis is not too close to one of the cube directions, $\{001\}$, is usually called a Geometrically Necessary Boundary (GNB). We will refer to them, however, as planar boundaries (from their morphology), because although they exhibit significant lattice tilt, most of the dislocations of which they are composed are not geometrically necessary. In some load configurations, these boundaries lie nearly parallel to the primary slip planes, a fact we shall use later. The IDB's inhabit the space between the planar boundaries, as shown in Fig. 1. These two types of boundaries have been extensively studied in recent years, and we refer to the literature for further details. [Mughrabi, Ungar, Kienle and Wilkens(1986); Barlow, Bay and Hansen(1985); Pantleon and Hansen; Winther, Huang Hansen(2000); Hughes, Liu, Chrzan and Hansen(1997)]

2.2 Surface Structure.

In addition to the well known cell wall structures, the dislocations cause steps to appear when they exit the surface. Knowledge of the surface structure has an even more ancient history than that of the internal structure. For example, the existence of deformation bands were well known even before dislocations were discovered [Elam(1935)]. In recent years, however, the materials community (as distinct from the mechanics community) has not focused on the surface features. But the surface structure mirrors the total plastic strain sustained by the system, with only the negligible elastic strain not represented in the surface steps, so the surface structure characteristics must be a central feature of any theoretical description.

In early stages, the surface is composed of a remarkably uniform distribution of fine slip. The slip lines are long, can extend across the entire sample, and decrease slowly in length as deformation proceeds [Seeger(1956); Mader(1957)]. The height of the slip steps can be a few Burgers vectors to perhaps a few tens of Burgers vectors [Wilsdorf and Kuhlmann-Wilsdorf(1952); Noggle and Koehler(1957); Savage, Kramer and Levine(2001)]. After secondary slip begins (Stage II), the fine slip becomes localized in coarse slip bands [Seeger(1956); Mader(1957)]. See Fig. 2. The fine slip is still present, but becomes the fine structure in the slip bands. Figure 2 shows that within a band, the individual slip lines are separated by a few tens of nanometers, and are the order of a few nanometers high. This confirms earlier work by Noggle and Koehler (1957). As deformation proceeds, the slip bands thicken (apparently up to a critical width [Savage, Kramer and Levine (2001)]) and new bands are nucleated.

2.3 Time Bursts.

But the strain is not only localized in space, it is also localized in time. The burst character has been known, qualitatively, for decades from acoustic emission studies, but Pond has published a more quantitative study [Pond(1973)]. Pond's experiments show that after a burst event has occurred in a band in time of the order of .1 s, a relaxation takes place of the order of seconds, during which no new strain takes place in the band. This relaxation time of course depends on the rate of strain in the system. Neuhauser has written a general review of the earlier work in the time domain [Neuhauser (1983)]. (Some very beautiful quantitative acoustic emission results have recently been reported in ice, [Miguel, Vespignani and Zapperi (2001)] but the deformation of ice is idiosyncratic to that system. Thus, we simply note that ice studies have been made, and rely for metal information on the Pond/Neuhauser experiments.) It is not known whether these bursts correspond to the formation of a single slip line in the band, or to a few simultaneous correlated slip events within the band. Comparing Pond's results quantitatively to those of Noggle and Koehler, and to Kramer (definitely a dangerous thing to do), however suggests the latter. We have reported the burst time as 0.1 s, as given by Pond, but the burst time depends on a number of factors [Neuhauser (1983)]. We suspect that Pond's reported burst time is an artifact of

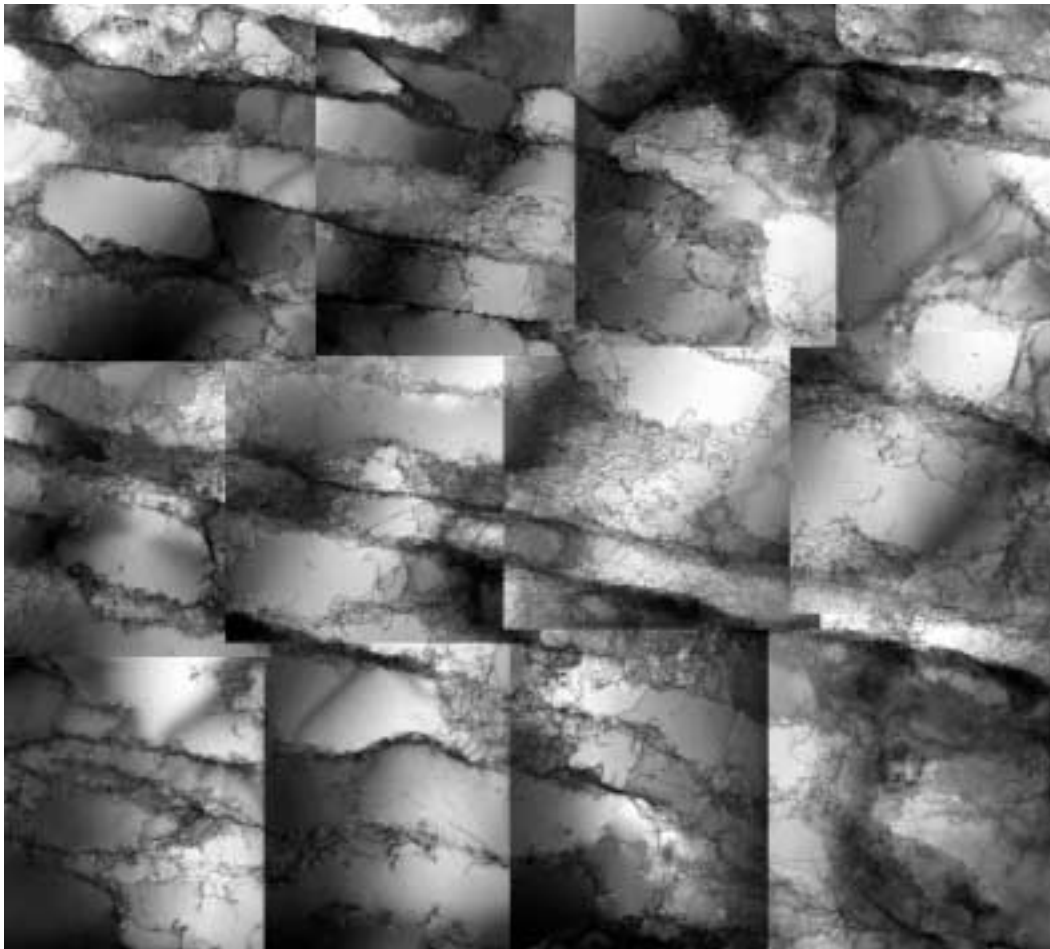
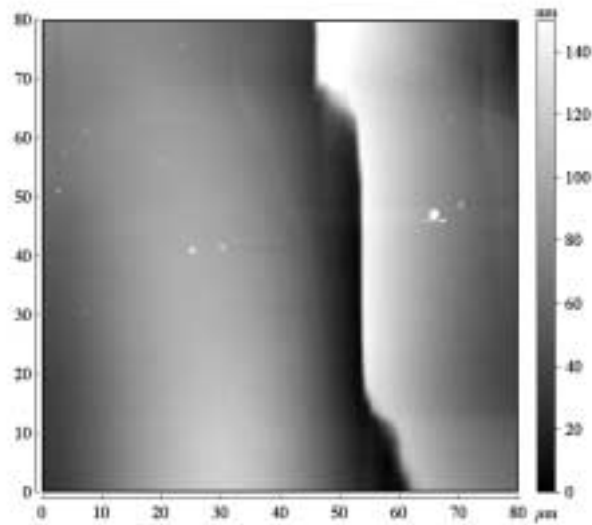
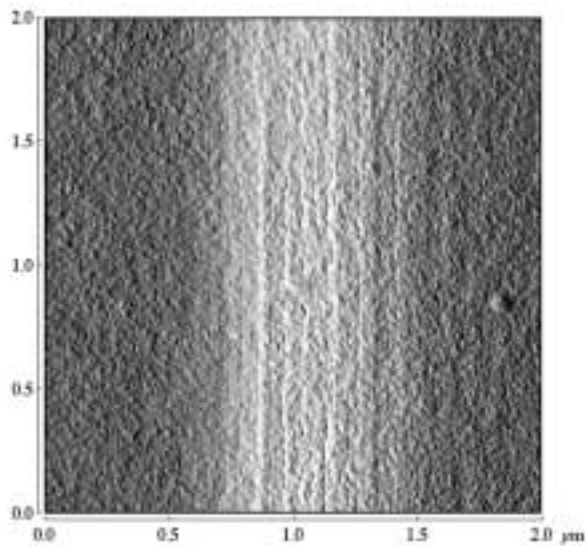


Figure 1 : A TEM view of Al deformed at 15% with load axis near [111]. Visible are long parallel walls (planar walls) and between them the smaller IDB cells.



(a)



(b)

Figure 2 : Surface structure on an Al single crystal deformed by a plastic strain increment of 1.5% as observed using atomic force microscopy. The loading axis was near [001]. Prior to this plastic strain increment, samples were deformed to a plastic strain of 15% and polished to remove the existing surface structure. a) Low magnification, showing parallel slip bands. b) Higher magnification, showing fine slip line structure within one of the slip bands. Individual slip steps are as high as 10 nm and are separated by as little as 40 nm.

his measurement method, and that the typical physical burst time may be considerably shorter than that.

From these comments, the central features of metal deformation are that it is characterized by the two classes of dislocation ordering, and by strain localization in both space and time.

3 Multiscale Modeling.

With these essential observational features in mind, in this section, we present a linked set of models, which extends from the level of dislocation dynamics to a continuum constitutive law. We present this linked list (with a brief summary of model details) with great tentativeness as a map, which we believe can be slowly filled out with realistic links as both theoretical and experimental studies provide the required details. As noted earlier, we do not address the mechanisms for the generation of the ordered dislocation structures, and assume that enough can be learned from experimentally known properties of the structures to make possible a meaningful theory.

3.1 Dislocation Dynamics.

In our scheme, dislocation dynamics is invoked to provide physical insight into the way strain is transmitted from one IDB cell to another. The strain transmission laws are parametrized in the percolation model, and the parameters and their dependence on the external stress and strain variables must be derived from some independent source. Experimental studies of the slip line structure can be expected to provide at least some of this information, but dislocation dynamics has unique capabilities for providing physical insight into the interplay between mobile dislocations and representative walls. We look forward eagerly to results from dislocation dynamics studies taking place under H. Zbib at Washington State University for input into the strain percolation model.

3.2 Strain Percolation Model.

In the strain percolation model, [Thomson and Levine(1998); Thomson, Levine and Stauffer (2000); Shim, Levine and Thomson] the IDB walls are assumed to act as both sources of, and barriers to, mobile dislocations. The percolation model is set up to track the transmission of strain from one cell to its neighbors when mobile dislocations pile up against a wall and trigger the

injection of new dislocations into neighboring cells. In the model, the strain transmission is determined by specifying rules for the transmission of strain from strained cell to neighboring unstrained cell, where these rules are couched in terms of parametrized probability distributions for dislocation sources in the walls. These percolation parameters are functions of the external stress and overall strain, and information on their functional form is obtainable, in principle, from atomic force microscopy (AFM) measurements of slip surfaces and the dislocation dynamics studies mentioned earlier.

In the model, in the space of the percolation parameters, two special phenomena occur. The first is the traditional geometrical percolation critical point, where for critical values of the parameters, the strained cluster grows from one side to the crystal to the other on a particular slip plane. Since the cluster at the critical point is fractal with a dimension less than two, the average strain per cell at the percolation threshold is zero in the infinite system size limit. See Fig. 3. But a second threshold exists,

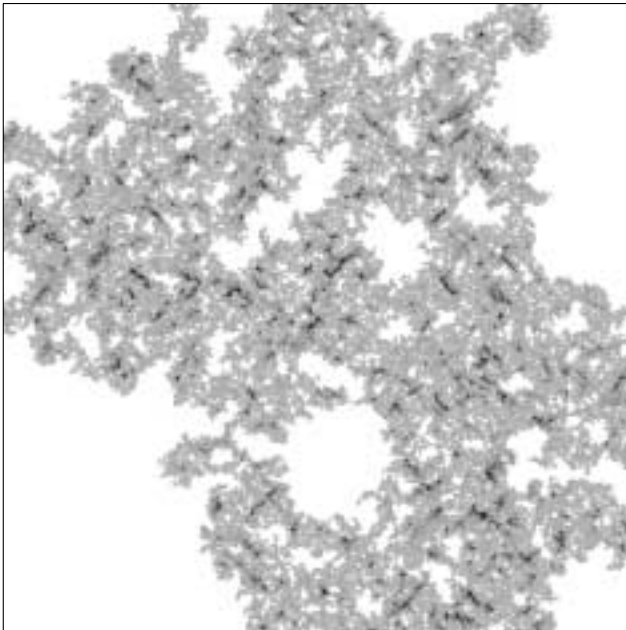


Figure 3 : Computer simulation plot of a strain cluster at the percolation critical point. Each point represents a strained cell, and the system is a square array of cells 1000 on a side. The grey scale indicates the magnitude of strain in the cluster, with darker regions denoting higher strain. The geometrical fractal dimension is 1.89.[Shim, Levine and Thomson]

where the system undergoes a strain avalanche, for parameter values somewhat above the geometrical percolation threshold. Between the percolation critical point and the strain avalanche point, the strain is a well behaved function of the percolation parameters. Since the average strain per cell is zero in the infinite size limit at the geometric percolation threshold, the physical system with its finite strain must correspond to parameter values in the super critical region just above the percolation threshold and below the strain avalanche point. In this super critical regime, the strain is actually physically constrained to be a few Burgers vectors in magnitude by the physically possible dislocation source mechanisms operating in the walls. For this reason, it is particularly important to obtain as much physical insight as possible into the wall behavior from dislocation dynamics studies. Contact with physical reality is achieved by postulating that the strain percolation model corresponds uniquely to one of Pond's burst events [Pond(1973)] wherein a single slip line is formed on the surface within one of the slip bands.

We have speculated that new percolation events are triggered by cross slip processes as the mobile dislocations are slowly absorbed into the walls during recovery after a percolation event has occurred. We have not pursued these ideas quantitatively, but we believe that combined experimental and theoretical studies of the slip line behavior can provide useful insight into the details of the relaxation mechanisms.

In summary, the percolation model describes the formation of elementary fine slip processes within a band. The model predicts reasonable values for the strain produced in each slip line burst event and is otherwise consistent with the known characteristics of the slip line geometry. But a theoretical treatment of the relaxation that occurs between percolation events has not been pursued quantitatively as yet.

3.3 Slip Line Localization.

Nothing in the percolation model provides a mechanism for spatial localization of the elementary slip lines into the slip bands, and for that we will outline a new proposed mechanism based on the channeling of percolation primary slip line events by the planar boundaries. The details of this mechanism will be presented elsewhere, but since it is new, we will provide here an outline of the ideas involved.

The localization mechanism is invoked for those load-

ing configurations where the planar boundaries lie nearly parallel to a single primary slip plane. When the load direction is near a crystallographic cube $\{001\}$ direction, no planar boundaries are produced at all, and when the load axis is near a $\{111\}$ direction, more than one set of planar boundaries is generated, so our focus is on the regions outside those limiting directions [Winther, Huang, and Hansen(2000)].

For this case, the space between the planar boundaries is filled by IDB cells. Since the planar boundaries are composed of very dense populations of dislocations, compared to the IDB walls, it is assumed that the planar boundaries form impenetrable barriers to the strain which percolates through the IDB's. But since the planar boundaries lie nearly parallel to the primary slip planes, let us focus on a pair of planar boundaries that are assumed to lie exactly parallel to such a slip plane. Since the planar boundaries exhibit significant lattice tilt across the boundary, the lattice outside the channel between the two walls will not be oriented in the channel configuration, and no percolating strain will be possible there. Thus in the assumed perfect channel, percolating strain can take place without interference from the barrier planar boundaries, and a slip band composed of many percolating slip lines can develop.

But any primary slip system will also generate some secondary slip on a different slip plane, and this strain, not lying parallel to the channel, cannot percolate. Such non percolating slip will be efficiently captured by the planar boundaries. It is natural to assume that these captured secondary dislocations are the ones which contribute the lattice tilt exhibited by the planar boundaries. If the boundary geometric tilt component is composed exclusively of these secondary dislocations, it will be a pure tilt boundary. But a pure tilt boundary in the fcc lattice is not parallel to one of the $\{111\}$ slip planes, and to rotate the boundary into the perfect channel configuration, a second set of dislocations must be included in the boundary. We will assume the second geometric component is composed of the primary slip dislocations. Figure 4 shows such a perfect channel between two planar boundaries with a tilt determined by the secondary dislocations, but rotated out of the pure tilt configuration by the primary dislocations. This boundary has zero long range stress.

We consider the effect of rotating the boundary slightly out of the perfect channel configuration. Now one set

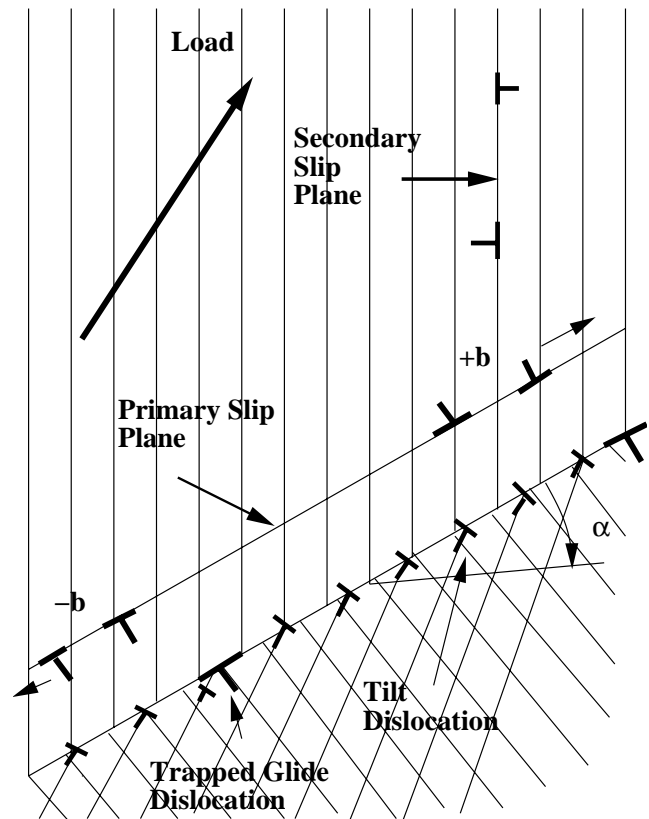


Figure 4 : A schematic drawing of a planar boundary parallel to a primary slip direction in an fcc lattice. Secondary dislocations formed during deformation are trapped by the boundary and are the main contribution to the lattice tilt across the boundary. But some primary dislocations are added to rotate the boundary from the pure tilt direction to the channel configuration.

of primary Burgers vectors will begin to collide with the lower boundary of the channel (shown in the figure), and those of opposite sign with the upper boundary (not shown in the figure). As these dislocations become incorporated into the boundary, the boundary will rotate back in the direction of the perfect channel configuration. This feed back mechanism stabilizes the slip band. It is likely that the channel will eventually saturate when it becomes filled with slip lines, consistent with recent AFM work at NIST [Savage, Kramer, and Levine(2001)].

The observed nucleation of new bands as deformation proceeds can also be understood on the basis of this mechanism. The “matrix” region between the bands is a region of nonpercolating slip. That is, even though slip cannot percolate through the matrix, one can expect considerable local slip activity to be taking place, and the planar boundaries that are observed throughout the deforming metal will interact with this localized slip. Occasionally, on a random basis, a local channel region will develop, and the feed back mechanism will “lock in” and create a new band of slip.

The statistics of channel formation is related to the problem of what degree of wandering of the channeling boundaries is permitted out of perfect registry. This is an important question when one realizes that the probability of finding a perfectly aligned channel must be zero in the infinite limit. So active physical channels must be permitted to statistically wander somewhat away from the perfect channel configuration. But the percolating slip plane will also wander from a perfect crystallographic plane because of the statistics of wall sources. So there will be an acceptance angle for channel wander, and this will be related to the probability of channel nucleation. These questions will be pursued further in a more quantitative manner elsewhere.

One further aspect of the channel mechanism is important to note. There are two time scales involved. The absorption of colliding secondary and primary dislocations will operate on the fast time scale appropriate to dislocation glide motion. But the rotation of a planar boundary must take place by recovery processes in the boundary, and this will be on a much slower time scale. That is, when either secondary or primary dislocations are first absorbed by any given planar boundary, these dislocations (and the boundary they form) will possess a long range stress field. It is only when the boundary is allowed to rotate by boundary atom rearrangement (and bound-

ary dislocation climb and glide) that the long range stress field can be minimized. The long range stress field is the boundary rotation thermodynamic driving force. So the mechanism we propose is a dynamic recovery process, and it will lead to important strain rate effects.

3.4 Continuum Constitutive Laws.

In the last two sections, we have overviewed the strain percolation model for the elementary fine slip features within a band, and a mechanism for the localization of that fine slip into the gross bands which appear on the surface. The output of the percolation model is the strain appearing in a fine slip step and the relaxation time between percolation events in a band (although we have not studied the relaxation time quantitatively yet). One output of the localization mechanism is the fact that there exist two separate regions with differing mechanical properties: the percolating slip band region, and the nonpercolating matrix between the bands. A second output of the localization mechanism is the nucleation rate of new bands out of the nonpercolating matrix region. There is experimental evidence that a minimum distance exists between adjacent slip lines, and there is a suggestion in AFM work at NIST that there may be a limit to the width of a band [Savage, Kramer, and Levine(2001)]. Both of these band characteristics need additional clarification.

With these outputs from the dislocation level models, one can infer the existence of a continuum level description with one hardening parameter suitable for slip band material and a second hardening parameter for the matrix material. We will present here a simplified scalar version of such a model to show how it is linked with the dislocation based models, and to illustrate the kinds of information it can supply.

We write the total strain, ϵ , as the sum of strain in the bands and that in the matrix,

$$\epsilon = r\epsilon_b + (1 - r)\epsilon_m, \quad (1)$$

where r is the volume fraction of the slip bands, and $\epsilon_b \gg \epsilon_m$. The macroscopic (mean field) hardening coefficient of the total system can be defined as

$$\frac{d\tau}{d\epsilon} = h_t, \quad (2)$$

where h_t is the slope of the total stress strain curve, and τ is the flow stress. Note that the macroscopic applied stress must be the same throughout the material,

and since we consider both bands and matrix to be deforming, even though the matrix is a minority partner, then the flow stress in both bands and matrix must be the same. So the different material properties of matrix and band must be expressed through different hardening coefficients. That is,

$$\begin{aligned} d\varepsilon &= rd\varepsilon_b + (1-r)d\varepsilon_m + (\varepsilon_b - \varepsilon_m)dr \\ &= \left(\frac{r}{h_b} + \frac{1-r}{h_m} \right) d\tau + (\varepsilon_b - \varepsilon_m) \frac{dr}{d\varepsilon}, \end{aligned} \quad (3)$$

where $d\varepsilon_b = d\tau/h_b$ and $d\varepsilon_m = d\tau/h_m$, and thus,

$$\left(1 - (\varepsilon_b - \varepsilon_m) \frac{dr}{d\varepsilon} \right) h = \frac{d\tau}{d\varepsilon}, \quad (4)$$

where

$$\frac{1}{h} = \frac{r}{h_b} + \frac{1-r}{h_m}. \quad (5)$$

In terms of the total hardening, $h_t d\varepsilon = d\tau$,

$$\begin{aligned} h_t &= h \left(1 - (\varepsilon_b - \varepsilon_m) \frac{dr}{d\varepsilon} \right) \\ &= \frac{h_m}{1-r+\alpha r} \left(1 - (\varepsilon_b - \varepsilon_m) \frac{dr}{d\varepsilon} \right). \end{aligned} \quad (6)$$

In the last equation, α is the hardening ratio, $\alpha = h_m/h_b \approx 10$.

The last equation is a general phenomenological relation. Experimentally, [Seeger(1956; Noogle and Koehler(1957))] as the deformation proceeds, the bands already formed fill with slip lines, and new bands are nucleated. Thus, r will be an increasing function of the overall strain, $r = r(\varepsilon)$, and the two hardening coefficients, h_b and h_m , will also be increasing functions of the total strain. This final equation thus has a general form which corresponds to the Voce curve of plasticity [Voce(1955)]. That is, the overall hardening, h_t , decreases with decreasing slope through Stage III.

Thus, not only is a two component model of the deforming solid consistent with surface slip observations, it is also consistent with the defining property of Stage III deformation that h_t decreases uniformly with strain. It has two main internal variables, r and α (in addition to h_m which sets the initial level of hardening at the beginning of Stage III).

4 Conclusions.

We have presented a linked set of models stretching, with no gaps, from the dislocation level to the continuum level. The links between models are the outputs from lower level models which become inputs for the higher levels. At the continuum level, a simple phenomenological two component model of the strain utilizes two main internal variables which are tied directly to features of the strain localization and percolation models.

Although we have certainly not yet worked out the full, or even a useable, version of the overall theory, we believe we have demonstrated the major features and important links of a plausible multiscale theory of metal deformation. Further, this demonstration suggests priorities for further work: The first is to understand better the band nucleation and evolution mechanisms. The second is to determine the relaxation mechanisms between bursts and the percolation strain hardening.

It must be said once more that the major lack in the proposed theoretical structure is that no mechanistic model yet exists for dislocation ordering and wall formation. In this scheme, we have assumed the wall structure characteristics are known, and built a transport theory on the basis of these known features. One will, of course, not be satisfied till this remaining ad-hoc aspect has been removed.

Acknowledgement: Robb Thomson gratefully acknowledges support from the Pacific Northwest National Laboratory operated by Battelle Columbus Corp.

References

- DeVincere, B. and Kubin, L.** (1994): *Modell. Simul. Mater. Sci. Eng.*, **2**, 559.
- Zbib, M.; Rhee, M.; and Hirth, J.** (1998): *Int. J. Mech. Sci.*, **40**, 113.
- Ghoneim, N.M. and Sun L.** (1996): *Phys. Rev. B*, **60**, 128.
- K. Schwartz** (1999): *J. Appl. Phys.*, **85** 108, 120).
- T. Ungar** (2001): "Dislocations 2000: An International Conf. on the Fundamentals of Plastic Deformation" *Mat. Sci. Eng. A*, **309-310**, 14.
- E. Zolotoyabko, D. Shilo and E. Lakin** (2001): "Dislocations 2000: An International Conf. on the Fundamentals of Plastic Deformation" *Mat. Sci. Eng. A*, **309-310**,

23.

D. Blavette, E. Cadel, A. Fraczkiewicz, et al. (1999) *Science*, **386**, 2317.

J. Th. De Hosson (2001): *MRS Abstracts*, Spring 2001, BB4.4 p. 449.

A.J. Wilkinson, M.B. Henderson and J.W. Martin (1996): *Phil. Mag. Lett.* **74**, 145-151.

J.-S. Chung and G. E. Ice (2000): *J. Appl. Phys.* **86**, 5249.

G. G. Long, L. E. Levine and R. Thomson (2000): *J. Cryst.*, **33**, 456.

P. Hahner (1996): *Appl. Phys. A*, **62**, 473.

A. El-Azab (2000): *Phys. Rev. B*, **61**, 11956.

M. Zaiser, “Dislocations 2000: An International Conf. on the Fundamentals of Plastic Deformation” in *Mat. Sci. Eng. A*, **309-310**, 304 (2001).

R. Thomson and L. E. Levine, *Phys. Rev. Lett.* **81**, 3884 (1998).

R. Thomson, L. E. Levine, and D. Stauffer, *Physica A***283**, 307, (2000).

Y. Shim, L. E. Levine and R. Thomson, *Mat. Sci. & Eng. A*, in press.

H. Mughrabi, T. Ungar, W. Kienle and M. Wilkens, *Phil. Mag. A*,**53**, 793 (1986).

C. Y. J. Barlow, B. Bay and N. Hansen, *Phil. Mag. A* **51**, 253 (1985).

W. Pantleon and N. Hansen, *Mat. Sci. & Eng. A*, in press.

G. Winther, X. Huang, and N. Hansen, *Acta Mater*, **48** 2187 (2000).

D. Hughes, Q. Liu, D. Chrzan, and N. Hansen, *Acta Mater*. **45**, 105 (1997).

C. Elam, *Distortion of Metal Crystals* (Oxford, Clarendon Press), (1935).

A. Seeger, “Dislocations and Mechanical Properties of Crystals”, Ed. J. C. Fisher, et al., Wiley (1956)

S. Mader, *Z. Phys.* **149**, 73, (1957).

H. Wilsdorf and D. Kuhlmann-Wilsdorf, *Z. Ang. Phys.*, **4**, 23 (1952).

T. Noggle and J. Koehler, *J. Appl. Phys.*, **28**, 53 (1957).

M. F. Savage, D. E. Kramer and L. E. Levine, *MRS Abstracts*, Spring 2001, BB4.4 p. 454 (2001).

R. B. Pond, Sr., in “The Inhomogeneity of Plastic Deformation”, p1, (1973) American Society for Metals Seminar Series, Metals Park, Ohio.

N. Neuhauser, *Dislocations in Solids*, ed. FRN Nabarro, vol 6, N. Holland, Amsterdam, (1983).

M. C. Miguel, A. Vespignani, S. Zapperi, et al., *Nature*, **410** 667 (2001).

Voce, E., *J. Inst. Metals*, **74** 537 (1948), *Metallurgica*, **51**, 219 (1955).

